http://dx.doi.org/10.15576/GLL/2022.3.131

GLL

Geomatics, Landmanagement and Landscape No. 3 • 2022, 131–146

GEOMATICS-BASED ASSESSMENT OF THE NEOTECTONIC LANDSCAPE EVOLUTION ALONG THE TEBESSA-MORSOTT-YOUKOUS COLLAPSED BASIN, ALGERIA

Hassan Taib, Chaouki Benabbas, Abdelkader Khiari, Riheb Hadji, Haythem Dinar

Summary

The neo-tectonic research is interested in the study of the movements of Earth's crust in recent geological times. It could explain the deformation mechanisms that lead to the structuring of drainage catchments. The Morsott-Tebessa-Youkous (Chabro) collapsed basin corresponds to a subsiding depression framed by brittle structures and filled with thick deposits. Our work aims to unveil the neo-tectonic activity and reconstruct the morphometric evolution of the landscape and the drainage network of the basin. For this task, our investigation applies a quantitative analysis of geomorphic indices extracted from the DEM of the study area. We used a GIS-based approach to compile seven morphometric factors namely Integral Hypsometry (HI), the Sinuosity of mountain fronts (Smf), the Valley Floor width to height ratio (VF), the Asymmetry Factor (AF), Basin Shape index (BS), and the topography (T). All these thematic parameters were processed in a Geo-database to calculate the study area's Relative Tectonic Activity Index (IRAT) as a result. The IRAT map was categorized into three classes. The result highlighted the distribution of relative tectonic activity in the region and unveiled some unknown faults. It associated the sinuosity of rivers and the deformation of the substratum with active tectonic anomalies. This research work succeeded in drawing up a new scheme of the neo-tectonic activity and morpho-structural evolution in the collapsed basin.

Keywords

tectonic activity • hypsometry index • sinuosity • asymmetry • topography

1. Introduction

The advent of geomatic acquisition technologies such as radar Interferometry, remote sensing, and drone imagery have significantly promoted scientific research in all fields of Earth Sciences [Hadji et al. 2014, a, b; Mouici et al. 2017]. Environmental water sciences, Geohazards, Structural geology, geomorphology, seismology, and neotectonics have seen their methodologies perfected by the adoption of new transversal approaches to

geodesy, geo-informatics, geochronology, and paleogeography... [Demdoum et al. 2015; Zahri et al. 2016; Hamed et al. 2017; Rais et al. 2017; El Mekki et al. 2018; Hamad et al. 2018; Ncibi et al. 2020]. Extremely difficult, costly, and time-consuming acquisition constraints of incision, erosion, slip, and uplift morpho-tectonic data were surpassed and have been significantly improved in coverage and accuracy [Dahoua et al. 2017; Anis et al. 2019; Nekkoub et al. 2020; Hamed et al. 2021]. The neotectonics based approaches are especially important in organizing land management and socio-economic development strategies in populated collapsed basins such as in our study area [Hamad et al. 2021]. The landform pattern of the mountain ranges and drainage basins are the results of the continuous competition between the pair (tectonics, erosion) [Mahleb et al. 2022]. This implies that tectonic activity is the predominant process in the genesis of the geological structures of the earth's crust [Kolata et al. 2010]. The configuration of the hydrographic networks in Neogene basins is thus shaped by the tectonic action. The methodological interpretation of landform measurable elements such as wadi incision, valley asymmetry, watercourse geometry, and stream deflections can trace the geological history and quantify the responses to dynamic action. Several proven researchers have used these geomorphic indicators to rate the tectonic activity in the deformed zone. Our adopted method has been applied worldwide and gave satisfactory results. It is the case, for example, of the North Rhine Graben [Peters and Van Baleen 2007], the middle of Zagros [Dehbozorgi et al. 2010], the southwest Sierra Nevada in Spain [El Hamdouni et al. 2008], and the East Cretan Cordillera of Spain [Pedrera et al. 2009]. The tellian belt is the result of the constant geodynamic evolution of the Tethysian margin by a set of tectonic events dating back to the Carboniferous/Palaeozoic extending from −358.9 ± 0.4 to −298.9 ± 0.2 million years. The pre-Miocene phase of the Alpine orogenesis gave rise to the Maghrebides orogenic chain [Wildi 1983; Vila 1980]. Numerous compressive, distensive, or strike-fault tectonic structures were set up since the upper Burdigalian. The Morsott-Tebessa-Youkous (Algeria), the extension of the Kasserine, Kalaa Djerad, and Sbiba-Cherichira (Tunisia) Mio-Plio-Quaternary collapsed basins highlight the perfect example of this orogeny [Khiari 1991; Tamani et al. 2019]. Our research aims to assess the behaviour of the most-easterly slumping basins of Algeria; based on the derivation of different geomorphic indices and the analysis of drainage shape. To achieve this objective; our study passes through three main steps: a) the extraction of the drainage network and geomorphic indices based on digital and topographic data. b) The preparation, rescaling, and geoprocessing, of these indices into a GIS platform, c) The combination of the seven dependent variables to yield the IRAT index. This study demonstrates the usefulness of the study of the morphotectonic features to trace back of the neotectonics activity of the North African collapsed basins and similar geological structures.

2. Geologic, geomorphic, and tectonic setting

The northeast of Algeria shows a complex Simo-tectonic and Morpho-structural setting, distinct by consequent seismic activity [Benabbas 2006]. The Neogene basins of northeast of Algeria are susceptible to developing several geologic hazards, especially

those related to the earth's movement [Manchar et al. 2018]. These phenomena become more complex when the impact of the geomorphic hazard intensifies in spatiotemporal scale [Mahdadi et al. 2018]. The study area belongs to Tebessa province, Northeast of Algeria between longitudes 3916246 to 3976415 N, and latitudes 926463 to 986767E (WGS 84, UTM 32N) (Fig. 1a). This transboundary basin is situated on the eastern edge of the Aures-Nememcha Mountain chain [Kowalski 1997]. The structuring of the region shows NE-SW fold axes and NW-SE grabens (Fig.1b). The lithostratigraphy is represented globally by gypsum-clayey Triassic diapirs of Jebel Jebissa and Belekfif, a thick limestone, and marls cretaceous in the borders of the basin, and a Mio-Plio-quaternary filling in the middle of the plain (Fig. 1c) [Kowalski et al. 2002].

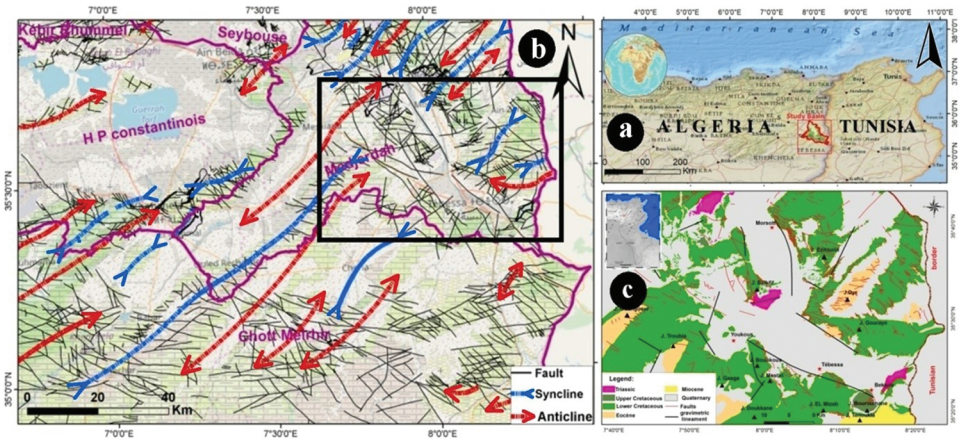

Source: Authors' own study

Fig. 1. a) Structural scheme of the study area, b) Geographic location of the study area, c) Stratigraphic simplified map of the study area

The Morsott-Tebessa-Youkous basin has been set up by the tectonic action of a nested fracture network. Lineaments showed three main sets of oriented faults NW-SE, NE-SW, and E-W, with the first predominant set in the study area, whereas the NW-SE and NE-SW fault sets have a homogeneous distribution [Boulemia et al. 2021]. The lineament and gravimetric analysis showed the ductile origin of the grabens and the covering of the major tectonic accidents by a quaternary filling [Brahmi et al. 2021]. The gravimetry confirms the existence of major NW–SE and NNW–SSE accidents between Morsott and Jebel Ezzitouna.

3. Material, methods, and data acquisition

The present study uses the topographic maps of Meskiana (N° 177), Morsott (N° 178), Youkous les Bains (N°205), and Tebessa (N° 206), a Shuttle Radar Topography Mission (SRTM) digital elevation model (DEM), and usual field measurements as the main data

acquisition for the research work. The DEM of 30 m resolution has been used for the extraction of morphometric indices and for basin delineation. Thus, the study area was subdivided into forty sub-basins. Geomorphic indices required to evaluate relative active tectonics and to calculate the IRAT-index including Hi, AF, Smf, VF, SL, BS, and T, were prepared [Esmaeil et al. 2017]. The ESRI-ArcGIS-10.6 and Xlstat-Pro software were utilized to digitize layers, execute statistics, and evaluate varied morphometric parameters in the study area. These thematic variables are processed, rasterized, and calculated within the GIS program. The field observations allowed us to sketch the fracturing shape in the limestone of the upper Cretaceous and the Eocene of Jebel Doukkane, and Jebel Mestiri.

4. Results, discussions, and data analysis

4.1. Geomorphic indices

For the detailed study of the morphotectonic features as described by Keller and Pinter [2002], and by using ArcHydro tools we have split the drainage catchment into forty sub-basins (Fig. 2b). For the generated sub-basins, we analysed seven geomorphic indices: hypsometric integral (HI), stream-length gradient (SL), fractal dimension (FD), basin asymmetry factor (Af), basin shape index (Bs), valley floor width to valley height ratio (Vf) and mountain front sinuosity (Smf). Then, as described by El Hamdouni et al. [2008] we combined these indices to characterize the active tectonics of the study area (Fig. 2e).

Asymmetric factor

The Af evaluates the tectonic tilting of a given drainage basin [Hare and Gardner 1985]. This factor is calculated based on geometric parameters according to the (1):

$$Af = 100 \cdot (Ar/At) \quad (1)$$

Ar is the area of the right side of the main catchment/watercourse, and at is its total area.

The values of Af are significantly controlled by the tectonic activity. If there is an orthogonal tilting versus the master water course direction; Af values become distant from fifty.

We have arranged the calculated Af values into three main classes, namely: symmetrical with ($Af < 5$), slightly asymmetrical with ($5 < Af < 15$), and strongly asymmetrical with ($Af > 15$). About 55% of valleys are characterized by a high asymmetry (Fig. 2a). The catchment N° 1, 4, 5, 7, 8, 13, 14, 21, 23, 27, 34, and 35 has Af values comprised between 17.20 and 37.24. Thus, the (NW-SE, E-W) and (NE-SW) normal faults coincide with the graben borders. Absolute values of asymmetry showed the large-scale tilting in the Tebessa Mountains.

Hypsometric analysis

The hypsometric analysis allows the determination of the morpho-structural mature-ness of the drainage basin based on its topography. Elevation data were acquired by digitizing equal contour intervals from topographic maps, backed by GPS surveys and

the DEM matrix. The HI combines the elevation data of the longitudinal profile of the main watercourse. Strahler [1952] defined HI as the relative portion of an area at different elevations, according to (2).

$$HI = (E_{mean} - E_{min})/(E_{max} - E_{min}) \quad (2)$$

Using Xlstat Pro, hypsometric curves are plotted by scaling the relative area as abscissa and relative height as ordinate. The mature basins are marked by low values of HI (< 0.4) and vice versa. The hypsometric analyses for the forty sub-watersheds of the study area show high to moderate integral values (HI close to 0.5) (Figs. 2 b, c, d) with a convex to sub-rectilinear shape. The HI curves could also quantize the erosion rate along the valley.

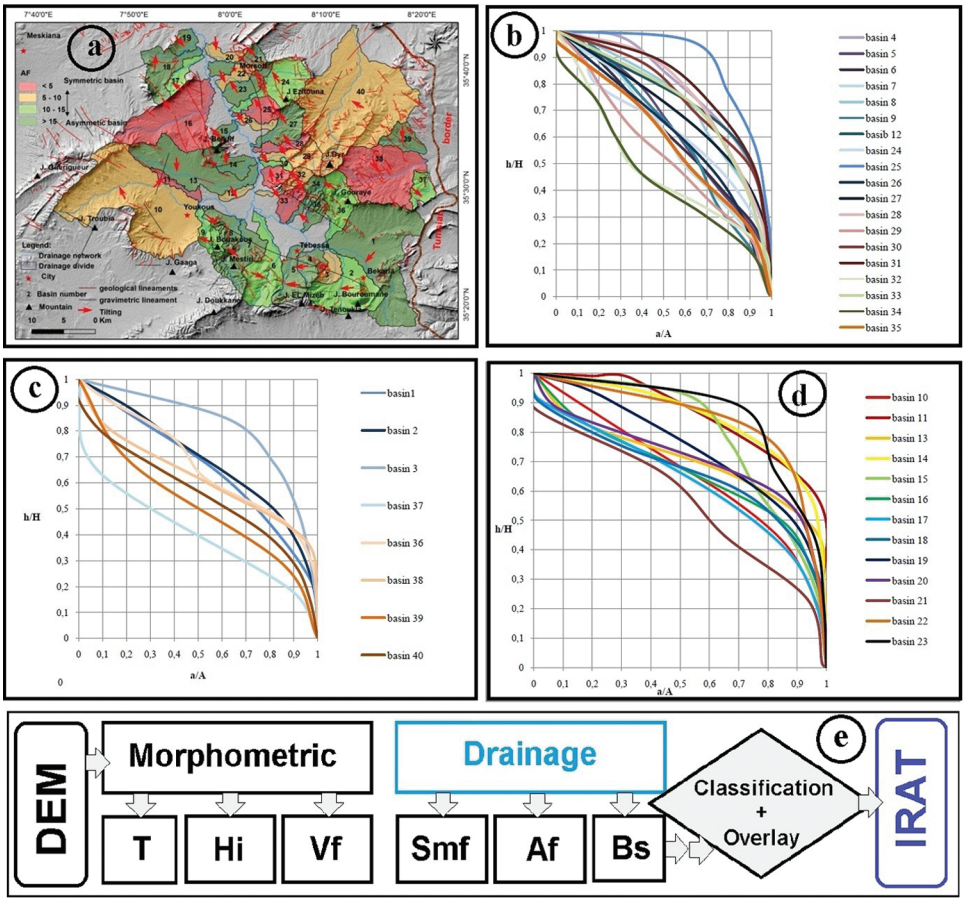

Source: Authors' own study

Fig. 2. a) Geomorphometric Asymmetry Index Distribution Map Af. b) Eastern hypsometric curves. c) Central hypsometric curves. d) Western hypsometric curves. e) Methodological flowchart of the adopted approach

Valley floor width to height ratio (Vf)

The valley floor width and valley height indices are used as informative parameters to assess tectonically active areas. Based on the DEM; we accomplished different transversal topographic profiles on the main watercourse valleys. Vf has been calculated as the ratio between the valley floor width and the valley height according to the (3) [Bull and Mc Fadden 1977]:

$$Vf = |2Vfw/(Eld + Erd - 2Esc)| \quad (3)$$

where:

Vf – the width of the valley floor,

Eld, Erd, and Esc – respectively: the altitudes of the left divide, the right divide, and the main watercourse.

If the value of valley floor width to height ratio is less than 1, the landscape is associated with linear rivers affected by a recent vertical movement, whereas for flat-bottomed valleys the Vf is >1, which indicates a base level of erosion. The calculated values of Vf (Fig. 3a) ranges between 0.02 (sub-basin N° 32) to 7.84 (sub-basin 10). This index is weak for V-shaped valleys and high for U-shaped valleys which are the case for most of the valleys in the study area (Fig. 3a).

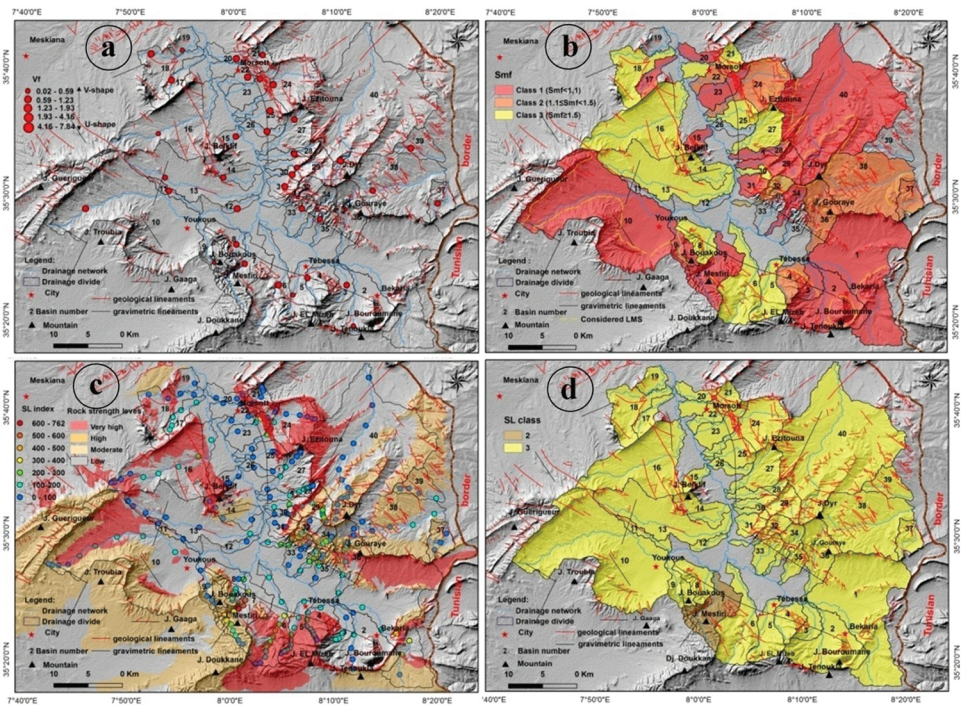

Source: Authors' own study

Fig. 3. a) Distribution map of the morphology index of (Vf). b) Mountain front sinuosity index map. c) The Rock Resistance and SL Map. d) SL Index Class Distribution Map

Mountain front sinuosity index (Smf)

The mountain sinuosity index is used to rate the relative tectonic activity alongside a given mountain front. In active zones, the uplift outperforms the erosion, shaping thus straight fronts. Low values (Smf < 1.5) highlight active mountain fronts whereas, high values (Smf > 3) shape inactive ones. The Smf index is calculated according to the (4) [Bull 2007]:

$$Smf = Lmf/Ls \tag{4}$$

where:

Lmf – the geometric break in the slope section,
Ls – the straight between two extremities of the mountain-front.

Excepting the sub-basin N° 21, the calculated Smf indexes do not exceed 1.28, which states that this zone is tectonically active (Fig. 3b).

Stream-length gradient index (SL)

The landform takes shape from a constant kinetic between the stream's erosional processes and tectonic action. The SL index is used to evaluate relative tectonic activity. A longitudinal stream profile, flowing on soft soils/rocks has a high SL index, indicating a recent tectonic activity. The SL index is calculated according to the (5) [Hack 1973]:

$$SL = (\Delta H)/(\Delta L)\ /L \tag{5}$$

where:

$(\Delta H)/\Delta L)$ – the slope gradient of the main watercourse segment,
L – the total length between the upstream and the mid of the watercourse segment.

To assess the effect of rock strength, we simply classified rock outcrops based on lithologic facies. Thus, we define four categories: low (silt, alluvium, and clay), moderate (clayey limestone, sandy siltstone), high (marly limestone), and extremely high (limestone) (Fig. 3c). According to El Hamdouni et al. [2008], we hierarchized SL indexes to three main classes: Class 1 (SL > 500), Class 2 (300 < SL < 500) and Class 3 (SL < 300). In our case, the SL values rages between 303.74 (basin N° 7), and 118.6 13.9 (basin N° 40) (Fig. 3d).

About 92% of the study area belongs to the class (3). The high values of SL are related to the resistance of limestone rocks, as the substratum of this part of the study area (Fig. 4c).

Drainage Basin Shape Index (Bs)

The drainage basin shape index is defined as the ratio of the basin length to the basin width at its widest point. It is calculated according to the (6) [Chang et al. 2015]:

$$Bs = Bl/Bw \tag{6}$$

where: Bs, Bl, and Bw – respectively the basin shape, length, and width.

The young drainage basins show an elongated shape due to their structuring in quiet tectonic processes. We divided the stretched values of BS into three main intervals: Class N° 1 (Bs > 2.9), Class N° 2 (1.9 < Bs < 2.9), and Class N° 3 (Bs < 1.9). In our case the basin N° 1 has the lowest Bs value (0.86) while the basin N° 28 has the highest Bs value (4.6) (Fig. 4a). About three-quarters of the study area belongs to the third class with almost circular shapes. While the remaining quarter individualizes in small, elongated basins (class 1 and 2), most of which are in the NE part of the area of Jebel Gouray, Ezitouna and Morsott.

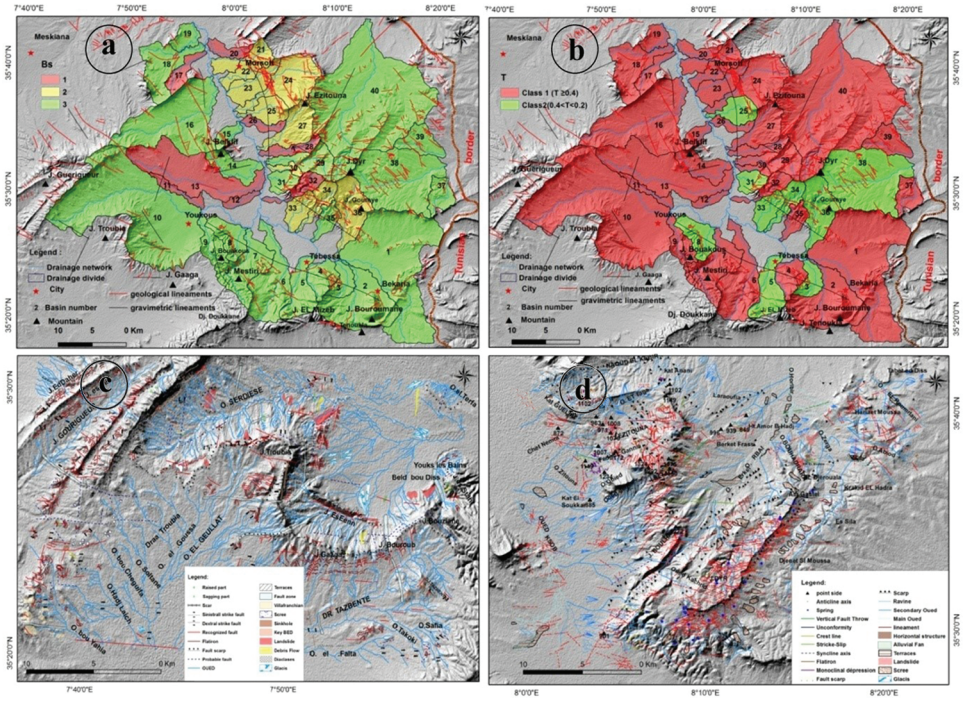

Source: Authors' own study

Fig. 4. a) BS index distribution map. b) T-index classes map. c) Morpho-structural map of the Youkous region. d) Morpho-structural map of the Morsot region

Transverse Topographic Symmetry Factor (T)

The T-Vector follows up on the variation of transverse topographic symmetry in various segments of a given valley. The T-factor index is calculated with the (7) [Cox 1994]:

$$T = Da/Dd \tag{7}$$

where:

Da – the distance from the midline of the drainage basin to the meander belt,
Dd – the distance from the basin midline to the basin divide.

We calculated the T-vector on 102 confluence points of the tributaries of the main watercourse. Then, we divided the obtained values into three classes: class N° 1(T > 0.4), class N° 2 (0.2 < T < 0.4), and class N° 3 (T < 0.2). The T-values disclose the symmetry of the valleys in most of the sub-watersheds of the study area (Fig. 4b).

4.2. Results discussion

The morphometric analysis has disclosed valuable insights into tectonic activity in the study area. The morpho-structural scheme pointed out an Atlassic structures with an East-west direction, dividing the study area into two main segments (Fig. 4c, d). The alternation of marl and limestone shaped an erosional landscape; especially in the cliffs of Jebel Guerigueur, and around Youkous valey. We have used the calcareous layers at the base of the Cenomanian as a marker level for the kinematics movement, the change of dip, and the continuation of stratigraphic layers. The dejection cones composed detritic glacis showed a wide range of forms, orientations, and material (Fig. 4d). They spread over the right bank of wadi El Ksob, North of Jebel Essenn and the borders of Youkous valley (Fig. 4c and 4d). These dejection cones are obvious through the migration of the hydrographic network towards the North. The shape of El Ksob wadi reveals the recent ditch activity (Fig. 4d). Numerous faults have been highlighted, most of which dive beneath the plio-quaternary formations of the basin valley.

4.3. IRAT evaluation

The relative tectonic activity index has been evaluated for the all the forty sub-basins, based on geomorphic and drainage indices. By using Geographic Information Framework Data (GIFD) procedure, the IRAT index has been generated by the combination of the hypsometric integral (HI), the asymmetry factor (AF), the stream-gradient index (SL), the ratio of valley floor width to valley height (Vf), the basin shape ratio (Bs), and the mountain front sinuosity (Smf) parameters (Table 1).

The result highlighted several anomalies in the drainage system, mountain fronts, and valley slopes. The morphometric anomalies have been determined from the VF and Hi index. Whereas the deviation of the hydrographic network from the T index. We also assessed the distribution of relative tectonic activity based on the active tectonic index (IAT).

The IAT has been calculated as the arithmetic mean of the Vf, Smf, SL, Af, Bs, HI, and T indices. This index was hierarchized into four main classes namely: extremely high tectonic activity (IAT < 1.5), high tectonic activity (1.5 < IAT < 2), moderate tectonic activity (2 < IAT < 2.5), and low tectonic activity (IAT > 2.5) (Fig. 5). On this map, the high and moderate IAT values spread on the whole of the basins, while low values typify solely the sub-basins N° 25 and 38.

Table 1. Values of morphotectonic indices for the forty subwatersheads and IAT classification

Basin	HI	AF	AF-50	BS	Mean SMF	Mean SL	Mean T	Vf	SL	BS	AF	HI	VF	T	SMF	S/n	IAT class	Assessen
1	0.5	12.75	–37.25	1.28	1.07	151.59	0.63	0.57	3	3	1	2	1	1	1	1.71	2	high
2	0.49	35.33	–14.67	0.86	1.09	100.69	0.45	1.12	3	3	2	2	2	1	1	2	2	high
3	0.47	55.12	5.12	1.83	1.07	93.78	0.23	3.75	3	3	2	2	3	2	1	2.2	3	Moderate
4	0.48	12.48	–37.52	1.29	1.11	122.29	0.82	2.72	3	3	1	2	3	1	2	2.14	3	Moderate
5	0.5	15.39	–34.61	2.21	1.24	135.36	0.38	1.,1	3	3	1	2	2	2	3	2.28	3	Moderate
6	0.5	63.09	13.09	2.28	1.28	205.76	0.52	6.42	3	3	2	2	3	1	3	2.42	3	Moderate
7	0.5	29.47	–20.53	1.41	1.04	303.74	0.56	2.64	2	3	2	2	3	1	1	2	2	high
8	0.5	75.69	25.69	1.43	1.21	127.83	0.3	2.86	3	3	1	2	3	2	3	2.42	3	Moderate
9	0.5	39.67	–10.33	2.24	1.01	99.8	0.57	0.59	3	3	2	2	1	1	1	1.85	2	high
10	0.5	40.35	–9.65	1.34	1.07	99.72	0.48	7.84	3	3	2	2	3	1	1	2.14	3	Moderate
11	0.49	48.86	–1.14	4.27	non	26.68	0.5	3.84	3	1	3	2	3	1	/	2.16	3	Moderate
12	0.48	58.88	8.88	3.48	non	17.62	0.81	6	3	2	2	2	3	1	/	2.16	3	Moderate
13	0.48	73.49	23.49	2.91	1.2	65.74	0.58	1.64	3	3	2	2	2	1	3	2.28	3	Moderate
14	0.47	68.11	18.11	2.02	1.21	53.57	0.56	2.36	3	3	2	2	3	1	3	2.42	3	Moderate
15	0.49	79.89	29.89	1.69	1.05	36.46	0.58	3.33	3	3	1	2	3	1	1	2	2	high
16	0.49	51.49	1.49	1.78	1.18	117.76	0.59	0.9	3	3	2	2	1	1	3	2.14	3	Moderate
17	0.47	39.1	–10.9	3.15	1.03	161.64	0.7	5	3	2	2	2	3	1	1	2	2	high
18	0.49	17.37	–32.63	1.67	1.17	59.1	0.65	7.63	3	3	1	2	3	1	3	2.28	3	Moderate
19	0.5	80.73	30.73	1.29	non	180.27	0.76	1.23	3	3	1	2	2	1	/	2	2	high

20	0.42	40.83	−9.17	3.14	1.07	37.9	0.59	5.66	3	2	2	2	3	1	1	2	2	high
21	0.5	74.09	24.09	2.24	1.85	84.55	0.54	3.5	3	3	2	2	3	1	3	2.42	3	Moderate
22	0.49	42.88	−7.12	1.9	1.12	65.83	0.53	5.71	3	3	2	2	3	1	2	2.28	3	Moderate
23	0.49	72.34	22.34	2.26	1.08	115.21	0.45	3.58	3	3	2	2	3	1	1	2.14	3	Moderate
24	0.5	63.76	13.76	1.92	1.13	180.27	0.52	5.4	3	3	2	2	3	1	2	2.28	3	Moderate
25	0.49	52.6	2.6	1.73	1.28	46.3	0.38	6.66	3	3	3	2	3	2	3	2.71	4	low
26	0.5	58.65	8.65	3.49	non	35.07	0.55	6.66	3	2	2	2	3	1	/	2.16	3	Moderate
27	0.49	77.9	27.9	2.26	1.19	79.51	0.59	2.12	3	3	1	2	3	1	3	2.28	3	Moderate
28	0.49	54.08	4.08	4.6	1.05	99.73	0.49	3	3	1	3	2	3	1	1	2	2	high
29	0.5	44.56	−5.44	1.65	1.09	244.99	0.47	1.93	3	3	2	2	2	1	1	2	2	high
30	0.46	39.45	−10.55	2.74	1.18	71.9	0.52	3.72	3	3	2	2	3	1	3	2/42	3	Moderate
31	0.47	53.37	3.37	1.44	1.03	30.85	0.23	5.4	3	3	3	2	3	2	1	2/42	3	Moderate
32	0.49	56.33	6.33	3.28	1.07	172.83	0.83	0.02	3	2	2	2	1	1	1	2	2	high
33	0.49	48.57	−1.43	1.77	non	72.47	0.32	2	3	3	3	2	2	2	/	2.5	3	Moderate
34	0.49	32.79	−17.21	2.86	1.04	161.51	0.39	0.47	3	3	2	2	1	2	1	2	2	high
35	0.5	85.97	35.97	1.93	non	100.48	0.4	1.75	3	3	1	2	2	1	/	2	2	high
36	0.5	61.13	11.13	2.14	1.14	115.63	0.37	0.5	3	3	2	2	1	2	2	2.14	3	Moderate
37	0.5	63.79	13.79	1.58	1,1	59.15	0.6	2.15	3	3	2	2	3	1	2	2.28	3	Moderate
38	0.5	52.48	2.48	1.5	1.15	91.28	0.29	4.16	3	3	3	2	3	2	2	2.57	4	low
39	0.5	78.49	28.49	1.26	non	68.25	0.59	4.7	3	3	1	2	3	1	/	2.16	3	Moderate
40	0.48	39.96	−10.04	1.34	1.09	13.9	0.41	5.71	3	3	2	2	3	1	/	2	2	high

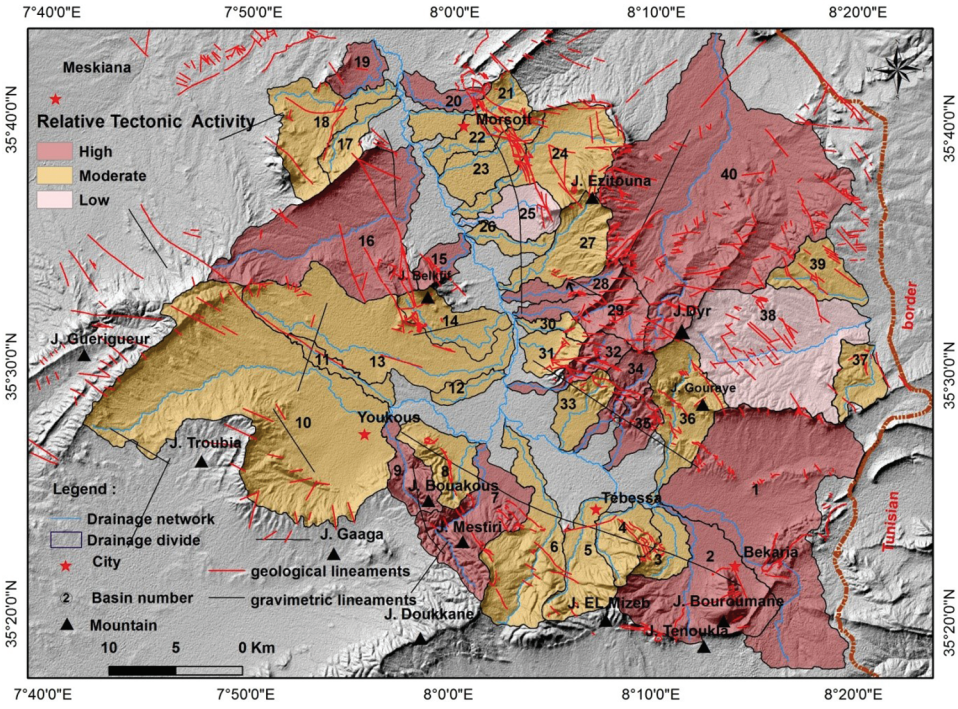

Source: Authors' own study

Fig. 5. Tectonic activity index (IRAT) map

5. Conclusions and outlook perspectives

Seismicity in the North-eastern Atlas is globally moderate. The tectonic has folded and faulted earth's crust since the Cenozoic by an Atlasic direction. Whereas the Neogene basins correspond to E–W elongation. Using GIS based-model, the Tebessa-Morsot-Youkous collapsed basin was divided into forty sub-watersheds; from where the analysis of seven morphometric indices (Hi, Sl, Vf, Smf, T, Af, and Bs) allowed the determination of the dynamic action, between the erosion processes, and the tectonic activity. The values of HI disclose the convex to the sub-rectilinear shape of basins. The high values of SL attest to the development of high fault zones in the mountain cliffs. The high values of VF indicate that the erosion process is existentially controlled by the relative tectonic activity. While the weak values of SMF indicate the prevalence of tectonic dynamics. Most values of Af prove the tectonic prevalence, whereas the values of Bs highlight high tectonic activity in the edges of the basin. The GIFD procedure has been adopted for the geospatial data processing of different morphometric parameters and for the calculation of the IRAT index. The resulting IRAT map highlights the relationship between tectonic Vs hydrology and tectonic Vs geomorphology. The

results are compliant with the observed structural activity. More information such as lithostratigraphic logs, interferometry remotely sensed data, and a high-resolution DEM is essential to quantify the detailed structural characteristics of the studied basin. The diachronic monitoring of the hydrographical network opens new perspectives to evaluate the effects of neo-tectonic and paleoclimate on the current evolution of the basin.

Acknowledgements

This work was overseen by the IAWRSMB – Tunisia and the Laboratory of Applied Research in Engineering Geology, Geotechnics, Water Sciences, and Environment, Setif 1 University, Algeria. Acknowledgments to the DGRSDT-MESRS for the technical support.

Conflicts of interest statement

On behalf of all authors, the corresponding author states that there is no conflict of interest. No participating authors have a financial or personal relationship with a third party whose interests could influence by the article's content.

References

Anis Z., Wissem G., Riheb H., Biswajeet P., Essghaier G.M. 2019. Effects of clay properties in the landslide's genesis in flysch massif: Case Aïn Draham, NW Tunisia. Journal of African Earth Sciences, 151, 146–152.

Benabbas C. 2006. Évolution Mio-Plio-Quaternaire des bassinscontinentaux de l'Algérienordorientale: apport de la photogéologie et analyse morpho structurale. Thèse de doctorat, Univ. Mentouri Constantine.

Boulemia S., Hadji R., Hamimed M. 2021. Depositional environment of phosphorites in a semiarid climate region, case of El Kouif area (Algerian-Tunisian border). Carbonates and Evaporites, 36(3), 1–15.

Brahmi S., Baali F., Hadji R., Brahmi S., Hamad A., Rahal O., ... Hamed Y. 2021. Assessment of groundwater and soil pollution by leachate using electrical resistivity and induced polarization imaging survey, case of Tebessa municipal landfill, NE Algeria. Arabian Journal of Geosciences, 14(4), 1–13.

Bull W.B. 2007. Tectonic Geomorphology of Mountains: A new Approach to Paleo Seismology. Hoboken, New Jersey, USA, Wiley-Blackwell.

Bull W.B., McFadden L.D. 1977. Tectonic geomorphology north and south of the Garlock Fault, California. In: Doehring D.O. (ed.). Geomorphology in Arid Regions: A Proceedings Volume of the 8th Annual Geomorphology Symposium, State University of New York, Binghamton, 23–24 September 1977, 115–138.

Chang Z., Sun W., Wang J. 2015. Assessment of the relative tectonic activity in the Bailongjiang Basin: Insights from DEM-derived geomorphic indices. Environ. Earth Sci., 74(6), 5143–5153.

Cox R.T. 1994. Analysis of Drainage Basin Symmetry as a Rapid Technique to Identify Areas of Possible Quaternary Tilt-Block Tectonics. Geological Society of America Bulletin, 106, 571–581.

Dahoua L., Savenko VY., Hadji R. 2017. GIS-based technic for roadside-slope stability assessment: a bivariate approach for A1 East-west highway, North Algeria. Mining Science, 24, 81–91.

Dehbozorgi M., Pourkermani M., Arian M., Matkan A.A., Motamedi H., Hosseiniasl A. 2010. Quantitative analysis of relative tectonic activity in the Sarvestan area. Geomorphology, 121(3–4), 329–341.

Demdoum A., Hamed Y., Feki M., Hadji R., Djebbar M. 2015. Multi-tracer investigation of groundwater in El Eulma Basin (North-western Algeria), North Africa. Arabian Journal of Geosciences, 8(5), 3321-3333.

El Hamdouni R., Irigaray C., Fernández T., Chacón J., Keller E.A. 2008. Assessment of relative active tectonics, southwest border of the Sierra Nevada (southern Spain). Geomorphology, 96(1–2), 150–173.

El Mekki A., Hadji R., Chemseddine F. 2017. Use of slope failures inventory and climatic data for landslide susceptibility, vulnerability, and risk mapping in souk Ahras region. Mining Science, 24.

Esmaeil H., Solgi A., Pourkermani M., Matkan A., Mehran A. 2017. Assessment of relative active tectonics in the Bozgoush Basin (SW of Caspian Sea). J. Mar. Sci., 7, 211–237.

Hack J.T. 1973. Stream-profiles analysis and stream-gradient index. Journal of Research of the U.S. Geological Survey, 1(4), 421-429.

Hadji R., Limani Y., Boumazbeur A., Demdoum A., Zighmi K., Zahri F., Chouabi A. 2014a. Climate change and their influence on shrink-age–swelling clays susceptibility in a semi-arid zone: a case study of Souk Ahras municipality, NE-Algeria. Desalin Water Treat.

Hadji R., Limani Y., Demdoum A. 2014b. Using multivariate approach and GIS applications to predict slope instability hazard case study of Machrouha municipality, NE Algeria. 10.1109/ICT-DM.2014.6917787 Publisher: IEEE Xplore. Accession Number: 14651190.

Hamad A., Hadji R., Bâali F., Houda B., Redhaounia B., Zighmi K., ... Hamed Y. 2018. Conceptual model for karstic aquifers by combined analysis of GIS, chemical, thermal, and isotopic tools in Tuniso-Algerian transboundary basin. Arabian Journal of Geosciences, 11(15), 409.

Hamad A., Hadji R., Boubaya D., Brahmi S., Baali F., Legrioui R., Abdeslam I., Hidouri B., Hamed Y. 2021. Integrating gravity data for structural investigation of the Youkous-Tebessa and Foussana-Talah transboundary basins (North Africa). Euro-Mediterranean Journal for Environmental Integration.

Hamed Y., Hadji R., Ncibi K., Hamad A., Ben Sâad A., Melki A., ... Mustafa E. 2021. Modelling of potential groundwater artificial recharge in the transboundary Algero-Tunisian Basin (Tebessa, Gafsa): The application of stable isotopes and hydro informatics tools. Irrigation and Drainage.

Hamed Y., Redhaounia B., Ben Sâad A., Hadji R., Zahri F. 2017a. Groundwater inrush caused by the fault reactivation and the climate impact in the mining Gafsa basin (SW Tunisia). J. Tethys, 5(2), 154-164.

Hamed Y., Redhaounia B., Sâad A., Hadji R., Zahri F., Zighmi K. 2017b. Hydrothermal waters from karst aquifer: Case study of the Trozza basin (Central Tunisia). Journal of Tethys, 5(1), 33-44.

Hare P.W., Gardner T.W. 1985. Geomorphic indicators of vertical neotectonism along converging plate margins, Nicoya Peninsula, Costa Rica. Tectonic Geomorphology, 4, 75-104.

Keller E.A., Pinter N. 2002. Active Tectonics. 2nd ed. Prentice Hall, Upper Saddle Rivers.

Khiari A. 1991. Etude comparative des structures du NE des Maghrébides et du SE du Caucase à l'aide du déchiffrement des images satellites. Thèse d'état, Univ. Lomonossov, Moscou, Russie.

Kolata D.R., Nelson W.J., Nimz C.K. 2010. Tectonic history. Geology of Illinois, 77-89.

Kowalski W.M., Hamimed M., Pharisat A. 2002. Les étapes d'effondrement des grabens dans les confines algéro-tunisiens. Bulletin du Service Géologique de l'Algérie, 13, 2, 131-152.

Mahdadi F., Boumezbeur A., Hadji R., Kanungo D. P., Zahri F. 2018. GIS-based landslide susceptibility assessment using statistical models: a case study from Souk Ahras province, NE Algeria. Arabian Journal of Geosciences, 11(17), 1-21.

Mahleb A., Hadji R., Zahri F., Chibani A., Hamed Y. 2022. Water-Borne Erosion Estimation Using the Revised Universal Soil Loss Equation (RUSLE) Model Over a Semiarid Watershed: Case Study of Meskiana Catchment, Algerian-Tunisian Border. Geotechnical and Geological Engineering, 1-14.

Manchar N., Benabbas C., Hadji R., Bouaicha F., Grecu F. 2018. Landslide Susceptibility Assessment in Constantine Region Algeria by Means of Statistical Models. Studia Geotechnica et Mechanica, 40(3), 208-219.

Mouici R., Baali F., Hadji R., Boubaya D., Audra P., Fehdi C.É., ... Arfib B. 2017. Geophysical, geotechnical, and speleologic assessment for karst-sinkhole collapse genesis in Cheria plateau (NE Algeria). Mining Science, 24, 59-71.

Ncibi K., Hadji R., Hamdi M., Mokadem N., Abbes M., Khelifi F., ... Hamed Y. 2020. Application of the analytic hierarchy process to weight the criteria used to determine the Water Quality Index of groundwater in the north-eastern basin of the Sidi Bouzid region, Central Tunisia. Euro-Mediterranean Journal for Environmental Integration, 5, 1-15.

Nekkoub A., Baali F., Hadji R., Hamed Y. 2020. The EPIK multi-attribute method for intrinsic vulnerability assessment of karstic aquifer under semi-arid climatic conditions, case of Cheria Plateau, NE Algeria. Arabian Journal of Geosciences, 13(15), 1-15.

Pedrera A., Pérez-Peña J.V., Galindo-Zaldívar J., Azañón J.M., Azor A. 2009. Testing the sensitivity of geomorphic indices in areas of low-rate active folding (eastern Betic Cordillera, Spain). Geomorphology, 105, 218–231.

Peters G., Van Balen R.T. 2007. Pleistocene tectonics inferred from the fluvial terraces of the northern Upper Rhine Graben, Germany. Tectonophysics, 430, 41-65.

Rais K., Kara M., Gadri L., Hadji R., Khochman L. 2017. Original approach for the drilling process optimization in open cast mines. Case study of Kef Essenoun open pit mine NE of Algeria. Mining Science, 24, 147-159.

Strahler A. 1952. Hypsometric analysis of erosional topography. Geological Society Bulletin, 63, 1117–1142.

Tamani F., Hadji R., Hamad A., Hamed Y. 2019. Integrating remotely sensed and GIS data for the detailed geological mapping in semi-arid regions: Case of Youks les Bains Area, Tebessa Province, NE Algeria. Geotechnical and Geological Engineering, 37(4), 2903-2913.

Vila J.M. 1980. La chaîne alpine d'Algérieorientale et des confinsalgéro-tunisiens. Thèse Univ. Paris VI.

Zahri F., Boukelloul M., Hadji R., Talhi K. 2016. Slope Stability Analysis in Open Pit Mines of Jebel Gustar Career, Ne Algeria. A Multi-Steps Approach. Mining Science, 23, 137–146.

PhD Hassan Taib
Department of Geology, Faculty of Earth Sciences and Architecture
Larbi Ben M'hidi University, Oum El Bouaghi, Algeria
Laboratory of Natural Resources and Management of Sensitive Environments, Algeria
e-mail: hacentaib8@gmail.com

Prof. Chaouki Benabbas
Geology and Environment Laboratory (L.G.E)
University of Constantine 3, Salah Boubnider, Algeria
e-mail: benabbas.chaouki@gmail.com

Prof. Abdelkader Khiari
Department of Geology, Faculty of Earth Sciences and Architecture
Larbi Ben M'hidi University, Oum El Bouaghi, Algeria
Laboratory of Natural Resources and Management of Sensitive Environments
e-mail: hhkhiari@yahoo.fr

Prof. Riheb Hadji
Department of Earth Sciences
Institute of Architecture and Earth Sciences
Laboratory of Applied Research in Engineering Geology, Geotechnics, Water Sciences and Environment, Ferhat Abbas University, Setif, Algeria
e-mail: hadjirihab@gmail.com
ORCID: 0000-0002-9632-0812

PhD Dinar Haythem
Department of Geology, Faculty of Earth Sciences and Architecture
Larbi Ben M'hidi University, Oum El Bouaghi, Algeria
Laboratory of Natural Resources and Management of Sensitive Environments
e-mail: dinarhaythem1@gmail.com